

Note to the Reader

To the best of our knowledge, this report documents all of the AC power transmission system data that is publicly available. If you are aware of other publicly available transmission system data, we would greatly appreciate it if you would bring those datasets to our attention.

For access, comments, or questions about the NESTA archive please contact the administrator: Carleton Coffrin, carleton@coffrin.com

NESTA

The NICTA Energy System Test Case Archive

Carleton Coffrin^{1,2,3}, Dan Gordon¹, and Paul Scott^{1,2}

¹Optimisation Research Group, NICTA

²College of Engineering and Computer Science, Australian National University

³Computing and Information Systems, University of Melbourne

September 29, 2022

Abstract

In recent years the power systems research community has seen an explosion of work applying operations research techniques to challenging power network optimization problems. Regardless of the application under consideration, all of these works rely on power system test cases for evaluation and validation. However, many of the well established power system test cases were developed as far back as the 1960s with the aim of testing AC power flow algorithms. It is unclear if these power flow test cases are suitable for power system optimization studies. This report surveys all of the publicly available AC transmission system test cases, to the best of our knowledge, and assess their suitability for optimization tasks. It finds that many of the traditional test cases are missing key network operation constraints, such as line thermal limits and generator capability curves. To incorporate these missing constraints, data driven models are developed from a variety of publicly available data sources. The resulting extended test cases form a compressive archive, NESTA, for the evaluation and validation of power system optimization algorithms.

Nomenclature

$V = v\angle\theta$	- AC voltage	θ^Δ	- Phase angle difference
$p + iq$	- AC power	f	- Fuel category
e	- AC current magnitude	μ	- Mean
y	- Line admittance magnitude	σ	- Standard deviation
$r + ix$	- Line impedance	λ	- Rate of an exponential distribution
b^c	- Line charge	e	- Exponential constant
t	- Line apparent power thermal limit	x^u	- Upper bound of x
$p^d + iq^d$	- AC power demand	x^l	- Lower bound of x
$p^g + iq^g$	- AC power generation	\hat{x}	- An estimation of x
c_0, c_1, c_2	- Generation cost coefficients	x	- A constant value
v	- Nominal voltage		

1 Introduction

Over the last decade, power systems research has experienced an explosion of publications applying operations research technologies to power network optimization problems, such as economic dispatch

[36], optimal power flow [34, 35], optimal transmission switching [18], and network expansion planning [25], just to name a few. Many of these publications have been inspired by new formulations of the AC power flow equations, such as the SDP/QC/SOCP relaxations [2, 23, 24] and the DC/LPAC/IV-Flow approximations [43, 9, 37], which bring industrial-strength general-purpose optimization techniques to AC power system applications.

Independent of the specific application or the power flow model under consideration, all of these works require AC power network data for experimental validation and it is important that realistic data is used to validate these applications and solution techniques. However, due to the sensitive nature of critical infrastructure, this kind of data is often very difficult to obtain. As a result, the research community most often uses a collection of power networks that are distributed with the MATPOWER research platform [54]. Many of these network models are over thirty years old [47]. They were originally designed to test the AC power flow problem, which is a feasibility task rather than an optimization task. Consequently, these test cases are missing key pieces of information, such as line thermal limits and generator cost functions, which are critical in optimization applications. Incorporating this missing information requires careful consideration, as it is easy to make test cases that are either trivial or infeasible.

This report has three goals: Firstly to conduct an extensive survey of all publicly available transmission system data sets and to curate them in one place with a consistent data format. Secondly, to make all of these test cases usable for optimization studies by reconstructing the missing data, and thirdly, to demonstrate that these completed test cases provide a valuable building block for developing new test cases tailored to specific application domains. The result is a comprehensive transmission network test case archive designed to be used for AC power flow optimization studies.

We begin, in Section 2, with a discussion of why the MATPOWER cases are inadequate for the study of optimization applications. We next conduct, in Section 3, a boarder survey of publicly available network data. Recognizing that the majority of test cases are missing key pieces of information, Section 4 proposes data driven approaches for reconstructing this information for the available test cases. Finally, in Section 5 we develop new test cases, and demonstrate that they are indeed interesting for testing optimization applications. Section 6 concludes the report.

2 Motivation

To better understand the MATPOWER test cases and keep this report within a reasonable scope, we focus on the seminal power network optimization problem: AC Optimal Power Flow (AC-OPF) [34, 35]. The AC-OPF problem is a continuous non-convex optimization problem and like many AC optimization problems, it can be shown to be NP-hard [51, 27, 30]. To address the computational difficulty of the AC-OPF problem, convex relaxations have been proposed [2, 23, 24, 15] as computationally efficient alternatives to the AC power flow equations.

For any given AC-OPF test case, we can measure the difficulty of the problem by comparing a heuristic solution of the true problem to lower bounds obtained by convex relaxations. Challenging test cases exhibit a large *optimality gap*, that is the relative difference between the objective value of the heuristic and relaxation as in (1).

$$\frac{\text{AC Heuristic} - \text{Relaxation}}{\text{AC Heuristic}} \quad (1)$$

To investigate the difficulty of the AC-OPF problem on the MATPOWER test cases, we compare, in Table 1, the following five variants of the AC-OPF problem,

1. AC – a heuristic solution to the full non-convex problem
2. CP – a *copper plate* relaxation which ignores all of the network constraints
3. NF+LL – a network flow relaxation incorporating a convexification of line losses [11]
4. SOC – the second-order cone relaxation [24]
5. SDP – the semi-definite programming relaxation [2]

The first four results were computed using IPOPT 3.12 [52] and the fifth result comes from a state-of-the-art SDP-OPF implementation [28] using the SDPT3 4.0 [46] solver. Note that the copper plate model cannot be applied to a few networks because they feature negative r and x values.

Test Case	\$/h AC	Optimality Gap (%)			
		CP	NF+LL	SOC	SDP
case4gs	17318.30	0.99	0.05	0.00	0.00
case5	17551.89	15.62	14.55	14.54	5.22
case6bus	3844.12	0.33	0.01	0.00	0.00
case6ww	3143.97	3.10	0.81	0.63	0.00
case9	5296.69	1.52	0.17	0.00	0.00
case14	8081.53	5.43	0.20	0.08	0.00
case24_ieee_rts	63352.20	3.71	0.36	0.01	0.00
case30	576.89	2.03	0.69	0.57	0.00
case_ieee30	8906.14	6.32	0.24	0.04	0.00
case39	41864.18	1.43	0.08	0.02	0.00
case57	41737.79	1.75	0.25	0.06	0.00
case89pegase	5819.81	1.50	0.36	0.17	err.
case118	129660.69	2.86	0.35	0.25	0.00
case300	719725.08	—	0.34	0.15	0.00
case1354pegase	err.	n/a	n/a	n/a	n/a
case2383wp	1868511.78	5.35	1.38	1.05	0.37
case2736sp	1307883.11	2.44	0.46	0.30	0.00
case2737sop	777629.29	1.75	0.39	0.25	0.00
case2746wp	1631775.07	3.09	0.53	0.32	0.00
case2746wop	1208279.78	2.50	0.56	0.37	0.00
case2869pegase	133999.84	1.16	0.19	0.09	err.
case3012wp	2591706.52	—	4.92	0.78	err.
case3120sp	2142703.73	—	5.20	0.53	err.
case3375wp	7412030.61	—	1.74	0.26	err.
case9241pegase	err.	n/a	n/a	n/a	n/a

Table 1: AC-OPF Bounds on the MATPOWER Test Cases.

The results for the copper plate model indicate that the network flow constraints typically only increase the AC-OPF objective by 2%–5% in these test cases. If line losses are incorporated (i.e. NF+LL and SOC), then the optimality gap can be reduced further, to less than 1% in most cases. Applying the more computationally expensive SDP relaxation indicates that these heuristic solutions are near global optimality for all but one of the test cases, as first observed in [27]. It is also interesting to note that [11] showed NF+LL is also a relaxation of the AC Optimal Transmission Switching problem (AC-OTS), indicating that these test cases are trivial for that optimization problem as well.

2.1 A 3-Bus AC-OPF Case Study

The small optimality gaps observed in the previous section suggests that the non-convex nature of the AC-OPF problem is not a major issue in the MATPOWER test cases. To illustrate that small optimality gaps are not a fundamental property of the AC-OPF problem, this section develops a simple 3-bus test case with significant optimality gaps. It also illuminates how the optimality gaps are sensitive to the input data, specifically line thermal limits and generator cost functions.

The three-bus power system is depicted in Figure 1 and the associated network parameters are presented in Table 2. This network is designed with a distant cheap generator at bus 1 and an expensive generator at bus 3, which is co-located with the load. The cheapest solution delivers as much power as possible from generator 1 and as little as possible from generator 3. Based on the network demand of 100 MW, we can observe that the cost of any AC-OPF solution is within the range of \$100–\$1,000. The AC-OPF solution is presented in Table 3. Without any binding constraints, all of the load is served from

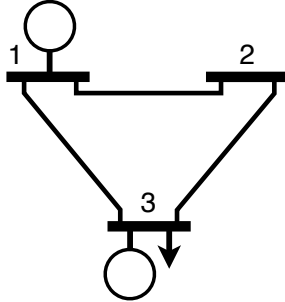


Figure 1: 3-Bus Example Network Diagram.

Bus Parameters					Line Parameters				
Bus	p^d	q^d	v^l	v^u	From-To bus	r	x	b^c	t
1	0	0	0.9	1.1	1-2	0.00	0.05	0	∞
2	0	0	0.9	1.1	2-3	0.00	0.05	0	∞
3	100	0	0.9	1.1	1-3	0.10	0.10	0	∞

Generator Parameters						
Generator	p^{gl}, p^{gu}	q^{gl}, q^{gu}	c_2	c_1	c_0	
1	0, ∞	$-\infty, \infty$	0	1	0	
3	0, ∞	0, 0	0	10	0	

Table 2: Three-Bus System Network Data (100 MVA Base).

Bus Values				Line Values		
Bus	p^g	q^g	v	Line	From MVA	To MVA
1	101	5	1.100	0.000	64	63
2	0	0	1.090	-1.434	63	63
3	0	0	1.080	-2.895	44	44

Table 3: Three-Bus System Solution.

the distant generator with a cost of \$101, with the small increase above \$100 being due to line losses.

The solution gets more interesting when binding network constraints (i.e. congestion) are introduced. We consider two congestion scenarios for this 3-bus example: (1) line capacity congestion, introduced by reducing the thermal limit of line 2-3 to 1 MVA and (2) voltage bound congestion, introduced by reducing the voltage range from ± 0.1 to ± 0.02 . Table 4 reports the cheapest generator dispatch across the different scenarios and power flow models. The table illustrates that the various power flow relaxations (CP, NF+LL, SOC, SDP) form a gradient of different accuracies, which are positively correlated with their computational difficulty. It should also be noted that by manipulating the generator costs (i.e. $c_{1,1}$, $c_{1,3}$), the optimality gap may be increased arbitrarily.

This 3-bus example is contrived, and such extreme cases are unlikely to occur in practice. One may wonder if the MATPOWER test cases exhibit small optimality gaps simply because they are more realistic. Upon a detailed investigation, we find that the small optimality gaps can be attributed to the following features of the networks:

1. Many of the line thermal limits are set to large non-binding values (i.e. 9900 MVA).
2. The synchronous condensers in some test cases were converted into active power generators.
3. Generators are assigned quadratic cost curves, often with the same coefficients.

Test Case	\$/h	Optimality Gap (%)			
		AC	CP	NF+LL	SOC
Capacity	985	89.84	88.93	88.93	1.32
Voltage	102	1.96	1.96	1.96	0

Table 4: AC-OPF Bounds using Relaxations on the 3-Bus Cases.

Throughout this report, we strive to produce test cases that are consistent with real-world data sources whenever possible. Interestingly, the resulting test cases strike a balance between the MATPOWER test cases and this extreme 3-bus example.

3 Publicly Available Network Data

Before proceeding further, it is important to survey and collect as many test cases as possible. To the best of our knowledge, Table 5 summarizes all of the readily available transmission system test cases. Given that many of these cases were originally designed for testing AC Power Flow algorithms, special care is taken to highlight the source of (or lack of) generation capacity limits, generation cost functions, and line thermal limits. Cells containing “—” indicate missing data, which must be added before the test case will be suitable for optimization applications.

In conducting this survey, some test cases were modified or omitted and a number of useful observations were made. The rationale for these modifications and omissions is as follows.

3.1 Network Modifications

Small Matpower Test Systems MATPOWER mostly contains test systems with sufficient data for AC-OPF studies. However, there are a few small cases with only enough data for AC power flow studies, namely, case4gs and case6bus. The following minor modifications are made to prepare these for AC-OPF studies.

1. case4gs – Generator costs are assigned similarly to the “cdf2mp” algorithm provided with MATPOWER, Pmax increased to 300 MW on the generator at bus 1, Qmax and Qmin are increased to 150,-150 MVar respectively to make the model feasible.
2. case6bus – Generator costs are assigned similarly to the “cdf2mp” algorithm.

Matpower 30 Bus Test System This test case was originally defined in [1] and latter modified in [17], with the later version being distributed with MATPOWER. The generator capacities and cost functions are significantly different in these two cases, hence we choose to include both using the identifiers *as* and *fsr* to differentiate the two cases.¹

EIRGrid Networks These test cases are provided in PSS/E-30 format and need to be converted into MATPOWER case files. The PSS/E file conversion tools provided with Pylon [33] and MATPOWER did not lead to converging AC power flows test cases on these networks. This may be caused in part to the explicit ΔY thirty degree phase shifts which are typically omitted from AC power flow studies [26] and several three winding transformers with negative resistance values. To address these challenges, we developed our own PSS/E-30 to MATPOWER translation tool, which produces converging AC power flow cases for these systems. However, these translations are only preliminary as we did not have access to PSS/E for verification of the translation. Detailed documentation of the translation process appears in the test case files.

¹The identifiers are based on the first initial of the authors’ last names.

Name	Original Source	Generator Capabilities	Generator Costs	Thermal Limits
IEEE Power Flow Test Cases				
14 Bus	[47]	—	—	—
30 Bus	[47]	—	—	—
57 Bus	[47]	—	—	—
118 Bus	[47]	—	—	—
300 Bus	[47]	—	—	—
IEEE Dynamic Test Cases				
17 Generator	[47]	—	—	—
IEEE Reliability Test Systems (RTS)				
RTS-79	[45]	[45]	[45, 40]	[45]
RTS-96	[21]	[45]	[40]	[45]
Matpower Test Cases				
case2383wp	[54]	[54]	[54]	[54]
case2736sp	[54]	[54]	[54]	[54]
case2737sop	[54]	[54]	[54]	[54]
case2746wop	[54]	[54]	[54]	[54]
case2746wp	[54]	[54]	[54]	[54]
case3012wp	[54]	[54]	[54]	—
case3120sp	[54]	[54]	[54]	—
case3375wp	[54]	—	[54]	—
PEGASE Test Cases				
case89pegase	[54]	[54]	—	[54], partial
case1354pegase	[54]	[54]	—	[54], partial
case2869pegase	[54]	[54]	—	[54], partial
case9241pegase	[54]	[54]	—	[54], partial
Edinburgh Test Case Archive				
Iceland	[6]	—	—	—
Great Britain	[6]	[6]	—	—
Reduced G.B.	[6]	[6]	—	[6]
EIRGrid Test Cases				
Summer Valley 2013	[14]	[14]	—	[14]
Summer Peak 2013	[14]	[14]	—	[14]
Winter Peak 2013-14	[14]	[14]	—	[14]
Publication Test Cases				
3-Bus	[31]	[31]	[31]	[31]
case4gs	[20]	[20]	—	—
case5	[32]	[32]	[32]	—
case6-ww	[53]	[53]	[53]	[53]
case6bus	[12]	—	—	—
case9	[13]	[54], original source unknown		
case30-as	[1]	[1]	[1]	[1]
case30-fsr	[1]	[17]	[17]	[1]
case39	[4]	[4, 38]	[16]	[41]

Table 5: Survey of Transmission System Data Sources

3.2 Network Omissions

IEEE 30 Bus “New England” Dynamic Test System This test case is nearly identical to the IEEE 30 test case and would not bring additional value to this archive.

IEEE 50 Generator Dynamic Test System In its specified state, this test case does not converge to an AC power flow solution. However, if the active generation upper bounds are increased to 1.5 times their given value, and voltage bounds are set to 1 ± 0.16 V p.u., then a solution can be obtained. This solution still exhibits significant voltage drops, atypical of other networks. Many of the lines in this network have negative r and x values, and it is unclear why. Also the size of the generating units are one or two orders of magnitude larger than any documented generation unit in the U.S. Due to these concerns, this network is omitted.

Networks for Optimal Transmission Switching A number of variants of the IEEE 118 [5] and IEEE RTS-96 [22] networks have been developed for use in optimal transmission switching studies. However, due to the difficulties with AC feasibility [11] we choose not to include them.

Local Minima Test Case Archive The University of Edinburgh, School of Mathematics has developed an archive of tests cases for the AC-OPF with known local minima [7, 8]. These test cases are very useful for testing AC-OPF algorithms, however, they are often significant departures from real-world inputs. In the interest of keeping this archive based on realistic test cases, we omit this local minima archive.

3.3 Network Observations

IEEE 300 Test System This test case exhibits very large voltage drops, with a voltage drop across branch 191–192 of 0.09 volts p.u. and 20 degrees. Such drops are not observed in the larger real-world networks [42], which brings the realism of this network into question. Also note that in the MATPOWER version of this network a phase shifting transformer is missing between buses 196 and 2040.

IEEE RTS-96 Note that RTS-96 [21] is simply three RTS-79 [45] networks connected together. One of the subtle points in these networks is the line charging on line 106–110, which is 2.459 p.u. In RTS-79, a -1.0 p.u. bus-shunt is used at bus 6 to balance out this massive line charge. This value must be used in all three analogous parts of the RTS-96 network to produce a feasible AC power flow. The generation costs presented in [21, 45] are not provided in \$/h, hence we adopt to interpretation of [40] to get them in the correct units.

3000 Bus Polish Test Cases Unlike the other Polish network cases, these test cases have 10 lines with negative resistance values. Hence, these lines can inject power into the network and invalidate some models, such as the AC copper plate relaxation. However, these negative values do not appear to adversely effect the power flow models considered in this report.

PEGASE Test Cases The Pan European Grid Advanced Simulation and State Estimation (PEGASE) Test Cases where originally studied in [19] and are now distributed with MATPOWER. The PEGASE cases with less than 9000 buses reflect an aggregated version of the Pan European Grid and hence have parameters that do not reflect individual network components (e.g. they include generators that can consume active power).

As indicated by Table 5, many of these networks are missing key information relating to generator capabilities, costs, and line thermal limits. We now turn to developing models to fill in the gaps in these test cases.

4 Data Driven Models

In an ideal situation, the data missing from Table 5 would be incorporated by returning to the original network design documents and extracting key specification information, such as generator nameplates and conductor specification sheets. Unfortunately, due to age of many of these test cases, the original sources are often unknown or inaccessible. A common approach for developing the missing data is to adopt simple equations, as exemplified by MATPOWER [54]. Drawing inspiration from the big data movement, we instead take a statistical approach built on publicly available datasets. Such data driven models may not reflect any specific real world network, but at least they reflect many of the statistical features found in real networks. As identified in Section 3, the key pieces of missing data are generator capability curves, generation costs, and line thermal limits. Throughout the rest of this section we analyze publicly available data sets, and propose data driven models that can fill the gaps in these test cases.

4.1 Generation Models

In classic AC power flow test cases, very little information is given about each generation unit. Typically, only the active power generation at one point in time and the reactive generation limits are provided. In contrast, optimization applications are best served by detailed models of the each generator's specification, including active/reactive power capability curves, ramp rates, startup/shutdown costs, and fuel efficiency. The challenge in building these generator models is to extrapolate reasonable operating capabilities from just one snapshot in time, that is, the operating point of the generator in the AC power flow case. To achieve this task, we first observe that the bulk of a generator's properties are driven by its mechanical design, which is in turn significantly influenced by its fuel type. Hence, we begin developing a data driven model for generators by assigning them a fuel category. Once a fuel category is determined, probabilistic models for both the active power capabilities and fuel costs of generators can be derived from publicly available data sources.

4.1.1 Reviewing the Data

The U.S. Energy Information Administration (EIA) collects vast amounts of data on generation units throughout the U.S. Two reports are particularly useful to this study, the detailed generator data (EIA-860 2012 [48]) and state fuel cost data (SEDS [49]). The fuel costs data is sufficiently summarized in the table, "Primary Energy, Electricity, and Total Energy Price Estimates, 2012" within SEDS. However, the generator data requires some processing before it can be used here.

Form EIA-860 provides detailed metadata for 19,000 generation units in the U.S. The key fields of for this study are status (e.g., operational, out of service, standby), energy source (i.e. the primary fuel type), Nameplate Capacity (MW), and Summer Nameplate Capacity (MW). We focus our attention on generators that are currently in service and have a single fuel type. This reduces the total number of generating units under consideration to 12,000. The EIA-860 form classifies generation fuel categories into detailed classifications, e.g., Residual Fuel Oil, Synthetic Gas, and Black Liquor (for a complete list see, [50]). We group these detailed classifications into the following broad categories: Coal (COW), Petroleum (PEL), Natural Gas (NG), Biomass (BIO), Nuclear (NUC), Dispatchable Renewables (DRN), and Renewables (RN). A complete mapping of fuel category codes is provided in Table 6. Before building

Fuel Category	Category Label	EIA-860 Labels
Coal	COW	ANT,BIT,LIG,SUB,WC
Petroleum	PEL	RC, DFO, JF, KER, PC, RFO, WO
Natural Gas	NG	BFG, NG, OG, PG, SG, SGC
Nuclear	NUC	NUC
Biomass	BIO	AB,MSW,OBS,WDS,OBL,SLW,BLQ,WDL
Dispatchable Renewables	DRN	WAT,GEO
Renewables	RN	SUN, WND

Table 6: Generator Fuel Category Mapping

the generation models, we elect to omit the Biomass, Renewables, and Dispatchable Renewables fuel categories for the following reasons.

1. RN – There is an implicit assumption in classic power system optimization problems that the generators are actively controlled via voltage magnitude and active power set-points. Hence, incorporating non-dispatchable generation is outside the scope of these problems.
2. DRN – To the extent that generation costs are modeled in this report, the marginal cost for fuel in renewable resources is considered to be 0. This may lead to a degenerate behavior in optimization problems studying nodal marginal prices. Dispatchable Renewables are omitted to avoid this degeneracy issue.
3. BIO – The generators within the biomass category are statistically quite similar to those in the petroleum category, and hence do not bring much additional value. This category is omitted in the interest of building a concise collection of fuel categories.

After filtering the fuel categories, 7,800 generation units remain from the previous set of 12,000. The following generator models are built using this filtered version of the EIA 2012 dataset.

4.1.2 Generation Fuel Category Classification Model

The first step in developing the generation unit models is fuel classification. Given that we have thousands of data points for generation units, it is possible to build an accurate empirical distribution of the data. We begin by sorting the generation units by their nameplate capacity. Observing that the nameplate capacities are not linearly distributed, we then break the data into contiguous bins containing at least 100 samples and build an empirical distribution from these bins, as in Figure 2. A fuel category classifier is easily built by selecting the corresponding nameplate capacity bin and rolling a weighted die to select the fuel type. When available, the fuel category classifier is applied on the maximum active generation value provided with the test case. However, when a maximum active generation value is unavailable, the current active generation value is a suitable alternative.

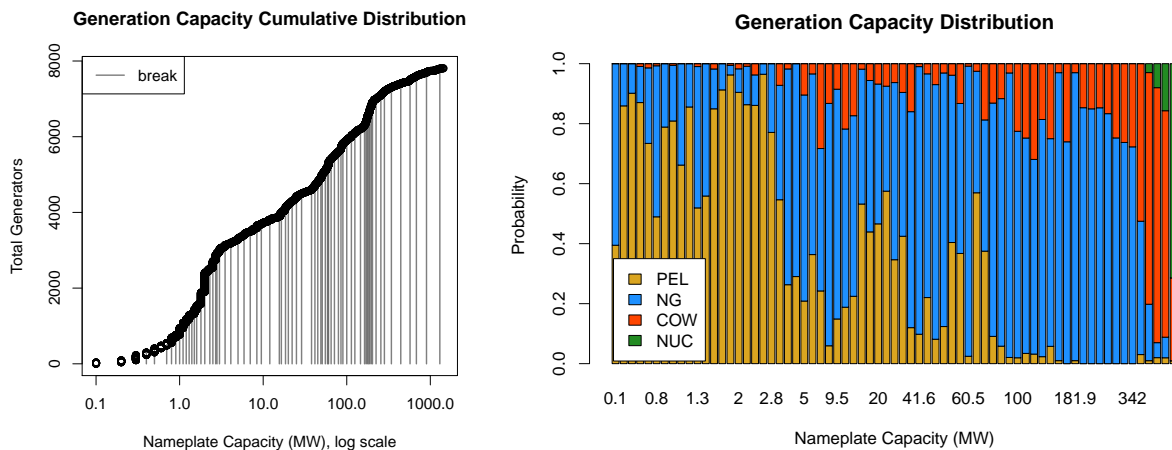


Figure 2: Distribution of Generator Nameplate Capacities (left), Empirical Distribution of Generation Fuel Categories (right).

One important point, which is easily overlooked, is the identification of synchronous condensers. In classic power flow studies such devices are not explicitly identified, and are modeled as voltage controlled generators with no active generation. To identify such devices, we introduce a new fuel category called SYNC, and any generator with an active generation upper bound of 0 is assigned this value. There is also one special case to be considered in generator category classification. Because many of these networks were originally designed as AC power flow test cases, the generators at the slack bus sometimes have no

active generation value specified, as this would be a free variable in a power flow study. If this occurs, we assume the generator is a very large and cheap power plant and assign it the class NUC. The empirical distribution shown in Figure 2 combined with these special cases forms the generation fuel classification model (GF-Stat).

4.1.3 Generation Capacity Models

An ideal generation capacity model would produce a complete generation capacity curve (e.g., Figure 15.8 from [26]). However, power system optimization models often approximate the generation capacity curve as a box by specifying upper and lower bounds on active and reactive power injection. We adopt this approximation and focus first on determining a reasonable upper limit on active power capabilities.

Active Generation Capability Before building statistical models for active generation capacities, the EIA data requires further filtering to be aligned with the existing test cases. Specifically, the EIA data contains many generators with less than 1MW nameplate capacity, in contrast over 90% of the generators in the test cases are above 1MW. To best capture the generators within in the available test cases, we remove generators below 5 MW from the EIA dataset resulting in a set of 4,500 units. The differences between these various distributions are summarized in Table 7.

	n	Quantiles, Capacity (MW)						
		Min	10%	25%	Median	75%	90%	Max
Test Case, Active Generation	910	0.1	2.4	15.8	76	271	313	2520
EIA, Nameplate Capacity	7808	0.1	1.0	2.0	16	94	233	1440
EIA, Nameplate Capacity ($\geq 5\text{MW}$)	4531	5.0	10.0	25.0	75	188	390	1440

Table 7: Active Generation and Nameplate Capacity Distributions

Grouping the active power nameplate capacity by fuel type, Figure 3 and Table 8 illustrate the clear differences across fuel categories. Notably, although each fuel category has a wide range of nameplate capacities, the medians of each fuel category are significantly different. Figure 4 further investigates the distributions within each fuel type and reveals that an exponential distribution is a suitable model for PEL, NG, and COW, while a normal distribution is suitable for NUC. The parameters from maximum likelihood estimation of these distributions are presented in Table 9. We also consider the the summer peak capacity reduction of each fuel category, as in Figure 5 and Table 9, to build a simple linear model for extreme cases when the more detailed probabilistic models fail.

Fuel Category	n	Quantiles, Capacity (MW)						
		Min	10%	25%	Median	75%	90%	Max
PEL	665	5	8	16	24	55	67	902
NG	2912	5	10	34	77	176	227	806
COW	852	5	12	75	200	556	720	1426
NUC	102	550	680	889	1127	1216	1289	1440

Table 8: Generator Nameplate Capacity Statistics by Fuel Category.

Combining all of these models, an active generation capacity model (AG-Stat) is constructed as follows. Given a fuel category f and an active generation upper limit or present output p^g , the fuel category nameplate capacity distribution is sampled as p^{gu} , until $p^{gu} > p^g$. The maximum active generation is then assigned the value of p^{gu} . However, if 100 samples are attempted and none satisfy $p^{gu} > p^g$, a last resort linear model based on summer peak reduction is used. It is assumed that p^g is the value of the generator running at the summer peak capacity and the maximum active generation is assigned as p^g increased to the appropriate nameplate capacity, as specified in Table 9.

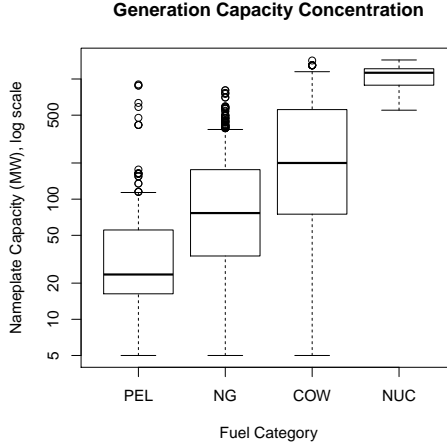


Figure 3: Distribution of Nameplate Capacities for each Fuel Category.

Fuel Type	Nameplate Capacity (MW)	
	$\hat{\lambda}$	Summer Reduc. $\hat{\mu}$
PEL	0.023254	16.11%
NG	0.009188	12.98%
COW	0.003201	8.48%

Fuel Type	Nameplate Capacity (MW)		
	$\hat{\mu}$	$\hat{\sigma}$	Summer Reduc. $\hat{\mu}$
NUC	1044.56	219.27	5.80%

Table 9: Distribution Parameters for Generator Capacity Models.

Reactive Generation Capabilities In synchronous machines, reactive generation capabilities are tightly coupled with active generation capabilities. Lacking detailed information about the generator’s specifications and having put significant effort into an active power capability model, simple models for reactive generation capabilities are developed. Using “Reactive Capability Curves of a Hydrogen Cooled Generator at Rated Voltage”, Figure 15.8, [26] as a guide, it is observed that the reactive power capability of a synchronous machine is roughly $\pm 50\%$ of its nameplate capacity. This inspires two reactive power models,

1. At Most 50 (RG-AM50) – This model assumes the given reactive power bounds are accurate, unless they exceed 50% of the nameplate capacity, in which case they are reduced to $\pm 50\%$ of the nameplate capacity. This provides a pessimistic model of the generator’s capabilities.
2. At Least 50 (RG-AL50) – This model assumes the given reactive power bounds are accurate, unless they are below 50% of the nameplate capacity, in which case they are increased to $\pm 50\%$ of the nameplate capacity. This provides an optimistic model of the generator’s capabilities.

These models are not often needed in this report, as the majority of cases studies come with reasonable reactive power bounds. However, such models are essential when developing significant departures from the standard test cases. For example, when developing test cases for long-term network expansion studies, where the reactive power capabilities can play an important role in the overall network design [3].

4.1.4 Generation Cost Model

Modeling generation costs could easily become a quagmire combining capital investment, game theory, agent modeling, and complex regulatory structures. However, like many classic power system optimiza-

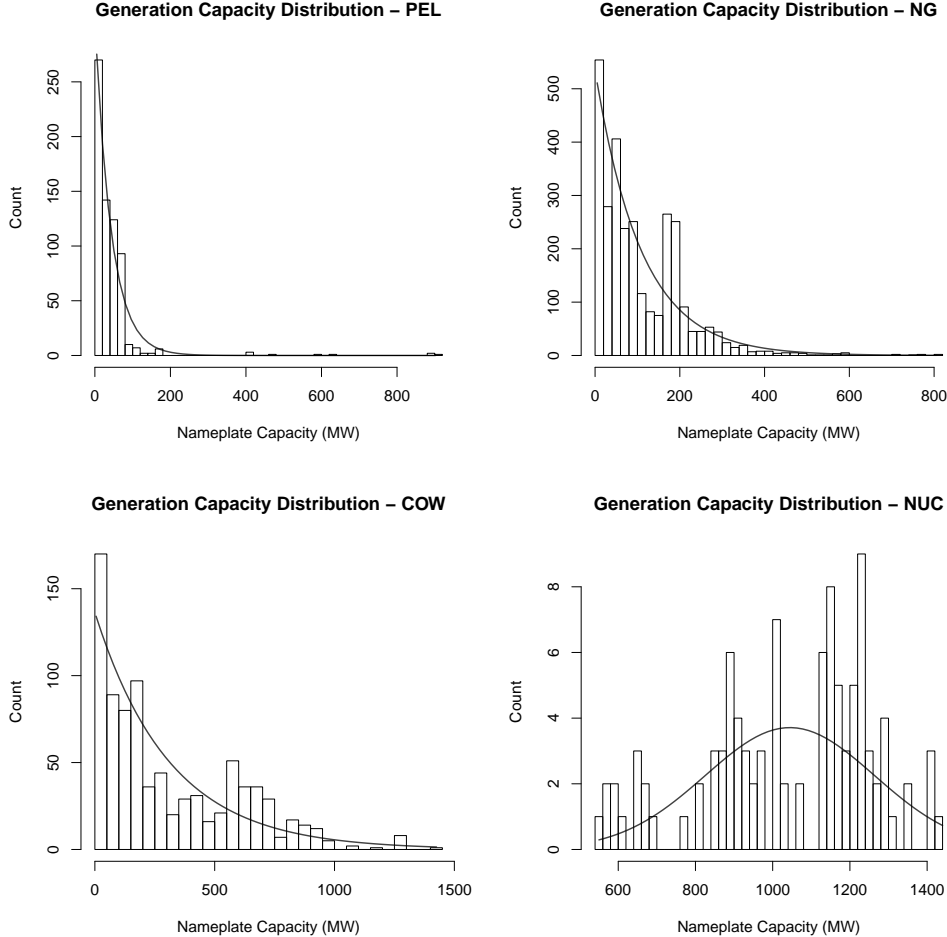


Figure 4: Distribution of Generator Nameplate Capacities with Probability Distributions.

tion problems (e.g., AC-OPF), we choose to avoid these modeling challenges by simply focusing on the marginal costs of power generation in a non-competitive environment. Namely, the entire network strives to minimize its cumulative fuel costs. We obtain fuel price information from “Primary Energy, Electricity, and Total Energy Price Estimates, 2012” in the SEDS dataset [49]. The SEDS fuel cost data is broken down by state and provided in Dollars per Million Btu. The conversion factor, 1 Million btu = 0.29307107 MWh, is used to convert these costs into appropriate units for a power system optimization problem. We observe that, for the fuel categories of interest, the fuel costs are roughly normally distributed, with the parameters specified in Table 10. The model for generation costs (AC-Stat) is built as follows. We assume that the fuel cost parameters from Table 10 are representative of the price variations across the various generating units, so that, given a fuel category, we simply draw a sample from the associated normal distribution to produce a fuel cost value. This value becomes the \$/MWh cost of that generator in the power system optimization problem.

At this point we have developed models for all of the key generation parameters, namely, active/reactive generation capabilities and generation costs. We now turn our attention to a transmission line thermal limit model, to complete the missing information for power system optimization.

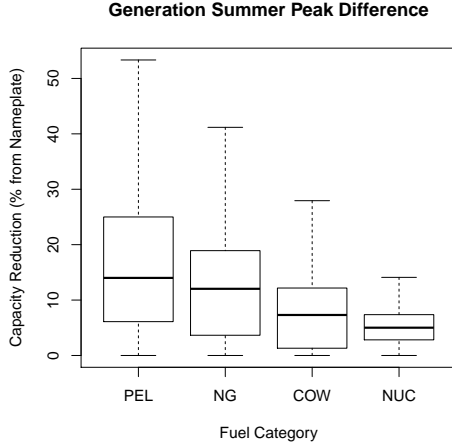


Figure 5: Distribution of Summer Peak Generation Capacity Reduction by Fuel Category.

Fuel Category	SEDS Label	Cost (\$/MWh)	
		$\hat{\mu}$	$\hat{\sigma}$
PEL	Distillate Fuel Oil	6.8828	0.3334
NG	Natural Gas	1.0606	0.2006
COW	Coal	0.7683	0.2452
NUC	Nuclear Fuel	0.2101	0.0199

Table 10: Generator Cost Model.

4.2 Thermal Limit Models

Determining a transmission line’s thermal rating is fairly straightforward when the conductor type and line length are available. Unfortunately, in all of the test cases studied here, none of this information is available. The only available line parameters are the impedance ($r + ix$ p.u.), line charge (b^c p.u.), and often the nominal voltage (\dot{v}) on the connecting buses. Given this limited information, it is common to estimate the thermal limit with a Surge Impedance Loading (SIL) [26, 29]. However, a significant shortcoming of this approach is that all of the lines within a given voltage level have the same thermal limit. This does not reflect real-world conditions, where lines have a wide range of thermal limits within each voltage level. This distinction is important for optimization applications, as it only takes one line with a low thermal limit to cause significant congestion in the power flow. In the rest of this section, a simple linear regression model is developed around the values of r , x and \dot{v} to go beyond SIL. Additionally, a reasonable upper bound for the line thermal limit is derived for cases where any of the r , x and \dot{v} values are available.

4.2.1 Reviewing the Data

Realistic line thermal limits are available from two sources, the Polish transmission system data provided with MATPOWER [54] and the Irish transmission system data provided by EIRGrid [14]. It was observed that these data sets do include a few lines without thermal limits, represented by large possessive numbers. These lines consisted primarily of transformers and lines below 20kV. To focus on meaningful data, we only consider lines that are not transformers, with thermal limits below 9.8 p.u., and nominal voltages below 250kV. After filtering, Figure 6 shows the line capacities of these networks broken down by kV Base. The mean capacity within each nominal voltage group clearly supports the SIL approach. However, the significant variance, which even leads to overlap between neighboring voltage levels, reaffirms the point that in real networks both low and high capacity lines exist for a given voltage.

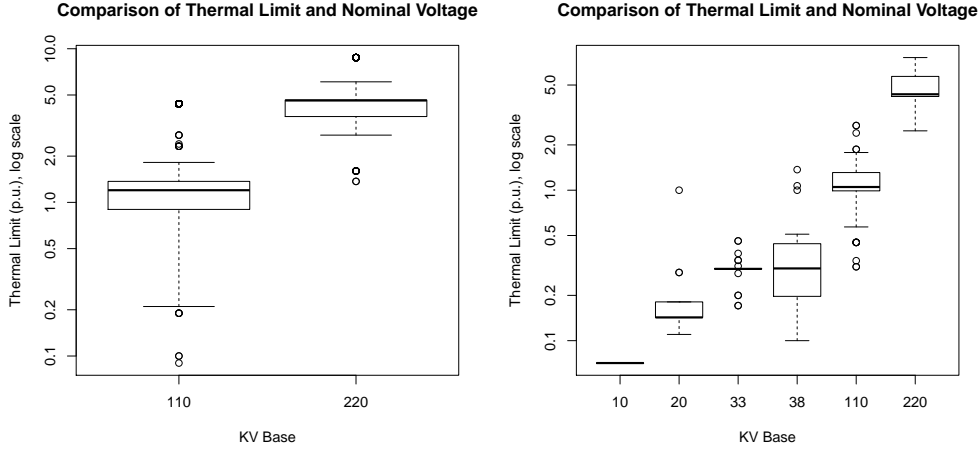


Figure 6: Polish Network case2383wp (left) and EIRGrid Summer Night Valley 2013 (right).

4.2.2 A Statistical Model

Our statistical model for line capacities was inspired by two key intuitions:

1. Thermal limits in AC power networks are typically given in terms of power flow (i.e. MVA), rather than current flow (i.e. MA). This leads to a property that conductors of the same type and configuration can have different MVA limits depending on their nominal voltage, despite the physical properties of the line being identical. If the MVA limits are converted to MA limits using the nominal bus voltage, equal conductors should have similar thermal limits.
2. The ratio of resistance to impedance may provide some insight into the line's conductor type and configuration, since this ratio should be independent of the line length, whereas the values taken individually will be proportional to the length.

After plotting these two values on a log scale, we observe a positive correlation, as illustrated in Figure 7. We then combine these two data sets in equal proportions (note that the Polish network produced 2600 data points while the EIRGrid network only produced 650), and fit a linear regression model to the log-log data, which fits parameters a and k in the following function,

$$y = e^a x^k \quad (2)$$

The fit log-log model and its parameters are presented in Figure 8. We recognize that this linear fit is fairly crude, however, the results in Section 5 demonstrate that it is sufficient for generating optimization test cases. It is also interesting to notice that the model selects $k = 0.4772$, which is nearly a square root. This is an encouraging result as thermal limits are closely related to heat dissipation and line losses, which increase quadratically with the line's current (i.e. $loss_{ij}^p = r_{ij}e_{ij}^2$).

This model (TL-Stat) can be used to estimate thermal limits in the following way. For any line with the necessary parameters, r , x , \dot{v} (on both sides of the line), the per unit thermal limit t is estimated as,

$$t = \dot{v} e^{-5.0886} \left(\frac{x}{r} \right)^{0.4772} \quad (3)$$

4.2.3 A Reasonable Upper Bound

Although the statistical model for line thermal limits is quite useful, it cannot be applied in cases where data for r , x , or \dot{v} is missing. Notable examples include: transformers, where the nominal voltage value differs on both sides of the line, and ideal lines, which do not have an r value. For these cases, it is helpful to have a method for producing reasonable upper bounds on the thermal limit. Typically, when no thermal limit is known, a large value is used in its place, such as 9.9 p.u. in the MATPOWER case and

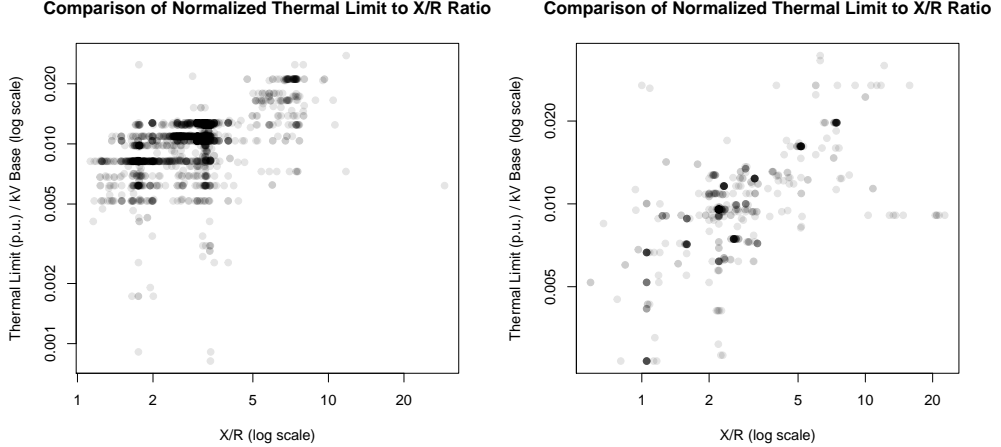


Figure 7: Polish Network case2383wp (left) and EIRGrid Summer Night Valley 2013 (right).

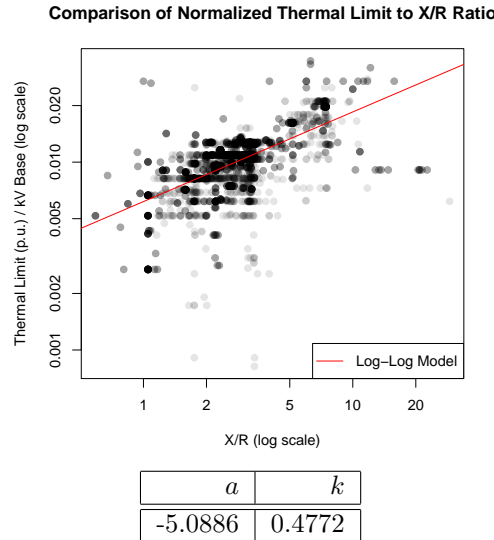


Figure 8: Linear Log-Log Model for equal proportions of data from the Polish Network case2383wp and EIRGrid Summer Night Valley 2013.

100.0 p.u. in the EIRGrid case. The key problem with this approach is that it most often deactivates the line thermal limit constraint and hides the true maximum throughput of the transmission line. Here we develop a theoretical approach for setting a line's thermal limit to a value that is close to the theoretical maximum but does not deactivate the thermal limit constraint, and which accurately indicates the line's true throughput limitations.

Recall that the thermal limit of a line is specified on the apparent power of the line, that is,

$$p_{ij}^2 + q_{ij}^2 \leq t_{ij}^2 \quad (4)$$

Our goal is to find a reasonable upper bound for t_{ij}^2 . Observe that the value of t_{ij}^2 can be stated in terms

of the the voltage variables as follows,

$$t_{ij}^2 = v_i^2 e_{ij}^2 \quad (5)$$

$$t_{ij}^2 = v_i^2 y_{ij}^2 |V_i - V_j|^2 \quad (6)$$

$$t_{ij}^2 = v_i^2 y_{ij}^2 (v_i^2 + v_j^2 - 2v_i v_j \cos(\theta_i - \theta_j)) \quad (7)$$

If we have reasonable bounds on $v_i, v_j, \theta_i - \theta_j$, then the task of determining the maximum throughput of a line can be stated as a numerical maximization problem where the objective is (7) and the constraints are the voltage bounds. However, given bounds on the voltage magnitudes ($\mathbf{v}^l, \mathbf{v}^u$) and the line's phase angle difference (θ_{ij}^Δ) we observe that the optimal point of this maximization problem is often,

$$t_{ij}^2 = (\mathbf{v}_i^u)^2 y_{ij}^2 ((\mathbf{v}_i^u)^2 + (\mathbf{v}_j^u)^2 - 2\mathbf{v}_i^u \mathbf{v}_j^u \cos(\theta_{ij}^\Delta)) \quad (8)$$

in realistic lines.² All AC networks have reasonable bounds on $\mathbf{v}^l, \mathbf{v}^u$ and recent studies [10, 42] have suggested 15° is a reasonable value for θ_{ij}^Δ . Combining these values with (8) we have a model for a reasonable upper bound on a line's thermal limit (TL-UB).

4.2.4 Validating the Models

To validate that both the statical and upper bound models are producing reasonable values, Figure 9 plots the correlation of the proposed MVA values to the real line thermal limits given in the Polish and EIRGrid networks. Both plots exhibit horizontal and vertical lines of points near the boundary of the figure, which are notable special cases. The collections of points forming horizontal lines around $y = 9.9$ p.u. and $y = 100$ p.u., are indicating missing thermal limits in the Polish and EIRGrid data respectively. The vertically aligned points around $x = 10000$ are a collection of lines with a very small reactance value modeling an ideal conductor, hence both models produce a value similar to positive infinity for their thermal limit. A perfect predictive model would place all of the points on the line $x = y$. The small clouds of points on that line in the left figure, indicate that the statistical model is producing reasonable values for many lines. In contrast, the upper bound model is consistently below the $x = y$ line, indicating it is in fact an optimistically high bound on the line's flow capacity, as it was designed to be.

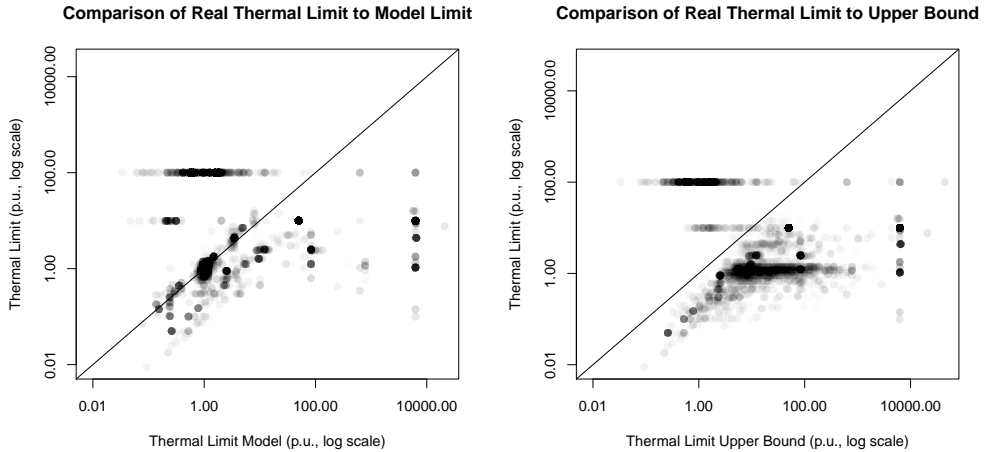


Figure 9: Comparison of the Statical Model (left) and the Thermal Limit Upper Bound Calculation (right) to the Given MVA Limits for Equal Proportions of the Polish Network case2383wp and EIRGrid Summer Night Valley 2013 (no data filtering used).

²The key assumption being that $2y \sin(\theta^\Delta/2)$ is large compared to $\mathbf{v}^u - \mathbf{v}^l$.

4.2.5 A Complete Thermal Limit Model

A robust thermal limit model (TL-Stat) is developed by combining the statistical model and the upper bound model in the following way. A line's thermal limit is computed with both the statistical model and thermal limit upper bound model (TL-UB) and the minimum of these two values is used. If the data required for the statistical model is unavailable on a given line, only thermal limit upper bound is computed. For test cases that include some line thermal limits, the model is applied only when it produces a tighter limit than the specified value.

5 The NESTA Networks

Now that we have built statical models for completing the missing data in the traditional test cases, we are ready to build the NESTA networks. In designing the NESTA networks we strive to keep the data as realistic and accurate as possible. Hence we only resort to using the statistical models when no realistic data is provided. Table 11 summarizes which models are used to convert existing test cases into NESTA test cases.

Recent research [10, 9, 23] has indicated that phase angle difference bounds may be valuable constraints for power system optimization. Hence all of the NESTA models have a generous phase angle difference bound of $\theta_{ij}^\Delta = 30^\circ$.

The statistical models were not applied to the PEGASE Test Cases for two reasons. First, due to the aggregation of network components, these statical models are less meaningful in these networks. And second, given the recent study of these networks in [19], there is significant value in keeping them relatively unchanged. It was observed that the phase angle bound and thermal limit models did not change the solution of these networks produced by MATPOWER.

Most of the time the NESTA test cases lead to feasible AC-OPF solutions, however, in a few cases it is necessary to override the statistical models to produce AC-OPF feasibility. The special overrides column in Table 11 indicates which networks require additional modifications. These modifications are detailed as follows:

IEEE 300 Bus Test Case As mentioned previously, this network exhibits atypical large voltage drops. As a result, the statistical line flow model (TL-Stat) is too constraining for this network. To ensure the network's feasibility, we resort to using the line flow upper bounds model (TL-UB) for the thermal limit on all of the lines.

Reduced Great Britain Test Case Many of the lines in this network have thermal limits well above the line flow upper bounds model. The model is used to assign reasonable values to these lines.

Great Britain Test Case At its default value, the thermal limit constraints on branches 599–592 and 2162–1868 make this model infeasible. Simply increasing these thermal limits to 800 and 50 MVA respectively resolves the issue and makes the network feasible.

Polish 3375 Winter Peak Test Case Unlike the other Polish network cases, this test case exhibits a number of strange features, including generators with unbounded reactive power capabilities and transmission lines without thermal limits. After applying the specified models, the following modifications are needed to make the test case feasible: The reactive capability of the first generator is increased to 4000 MVar to support a similar sized reactive load at bus 10079. Lines 10082–10079, and 10129–10130 have their thermal limits increased to 1000 MVA and lines 10330–10359 and 10331–10359 have their thermal limits increased to 250 MVA. Given the scale of this network, these modifications are quite minor.

5.1 Results

To verify the usefulness of NESTA for optimization applications we revisit the power flow relaxations from Section 2 in Table 12. In this table “err.” indicates the solver failed to converge while “—” indicates the model was not applicable to that input data. Note that CP relaxation cannot be applied to networks

NESTA Name	Original Name	Model						Special Overrides
		Active Gen.	Reactive Gen.	Gen. Cost	Thermal Limit	Phase Angle Bound		
IEEE Power Flow Test Cases								
nesta_case14_ieee	14 Bus	AG-Stat	RG-AM50	AC-Stat	TL-Stat	30°	—	
nesta_case30_ieee	30 Bus	AG-Stat	RG-AM50	AC-Stat	TL-Stat	30°	—	
nesta_case57_ieee	57 Bus	AG-Stat	RG-AM50	AC-Stat	TL-Stat	30°	—	
nesta_case118_ieee	118 Bus	AG-Stat	RG-AM50	AC-Stat	TL-Stat	30°	—	
nesta_case300_ieee	300 Bus	AG-Stat	RG-AM50	AC-Stat	TL-UB	30°	—	
IEEE Dynamic Test Cases								
nesta_case162_ieee_dtc	17 Generator	AG-Stat	RG-AM50	AC-Stat	TL-Stat	30°	—	
IEEE Reliability Test Systems (RTS)								
nesta_case24_ieee_rts	RTS-79	—	—	—	—	30°	—	
nesta_case73_ieee_rts	RTS-96	—	—	—	—	30°	—	
Matpower Test Cases								
nesta_case2383wp_mp	case2383wp	—	—	—	—	30°	—	
nesta_case2736sp_mp	case2736sp	—	—	—	—	30°	—	
nesta_case2737sop_mp	case2737sop	—	—	—	—	30°	—	
nesta_case2746wop_mp	case2746wop	—	—	—	—	30°	—	
nesta_case2746wp_mp	case2746wp	—	—	—	—	30°	—	
nesta_case3012wp_mp	case3012wp	—	—	—	TL-Stat	30°	—	
nesta_case3120sp_mp	case3120sp	—	—	—	TL-Stat	30°	—	
nesta_case3375wp_mp	case3375wp	—	RG-AM50	—	TL-Stat	30°	Yes	
PEGASE Test Cases								
nesta_case89_pegase	case89pegase	—	—	—	TL-UB	30°	—	
nesta_case1354_pegase	case1354pegase	—	—	—	TL-UB	30°	—	
nesta_case2869_pegase	case2869pegase	—	—	—	TL-UB	30°	—	
nesta_case9241_pegase	case9241pegase	—	—	—	TL-UB	30°	—	
Edinburgh Test Case Archive								
nesta_case186_edin	Iceland	AG-Stat	RG-AM50	AC-Stat	TL-Stat	30°	—	
nesta_case2224_edin	Great Britain	—	—	AC-Stat	TL-Stat	30°	Yes	
nesta_case29_edin	Reduced G.B.	—	—	AC-Stat	TL-UB	30°	—	
EIRGrid Test Cases								
nesta_case1394sop_eir	Summer Valley 2013	—	—	AC-Stat	TL-UB	30°	—	
nesta_case1397sp_eir	Summer Peak 2013	—	—	AC-Stat	TL-UB	30°	—	
nesta_case1460wp_eir	Winter Peak 2013-14	—	—	AC-Stat	TL-UB	30°	—	
Publication Test Cases								
nesta_case3_lmbd	3-Bus	—	—	—	—	30°	—	
nesta_case4_gs	case4gs	—	—	AC-Stat	TL-Stat	30°	—	
nesta_case5_pjm	case5	—	—	—	TL-Stat	30°	—	
nesta_case6_ww	case6ww	—	—	—	—	30°	—	
nesta_case6_c	case6bus	AG-Stat	RG-AM50	AC-Stat	TL-Stat	30°	—	
nesta_case9_wscc	case9	—	—	—	—	30°	—	
nesta_case30_as	30 Bus-as	—	—	—	—	30°	—	
nesta_case30_fsr	30 Bus-fsr	—	—	—	—	30°	—	
nesta_case39_epri	case39	—	—	—	—	30°	—	

Table 11: NESTA Instance Generation Details

with negative r, x values and that the SDP-OPF implementation does not support inactive buses (i.e. type 4 in MATPOWER), which occur in the EIRGrid test cases.

In Table 12, many of the best optimality gaps have remained small (i.e. below 1%). This is to be expected, as a number of the test cases were not modified significantly from their original form. However, if we focus our attention on the NF+LL results, a number of networks do exhibit significant optimality gaps, such as `nesta_case30_ieee`, `nesta_case162_ieee_dtc`, `nesta_case300_ieee`, and `nesta_case2224_edin`. This suggests that some benefits may be gained from solving the AC-OTS problem on these networks.

Test Case	\$/h AC	Optimality Gap (%)			
		CP	NF+LL	SOC	SDP
nesta_case3_lmbd	5812.64	2.99	2.26	1.32	0.39
nesta_case4_gs	156.43	29.69	7.01	0.00	0.00
nesta_case5_pjm	17551.89	15.62	14.55	14.54	5.22
nesta_case6_c	23.21	1.88	0.36	0.30	0.00
nesta_case6_ww	3143.97	3.10	0.81	0.63	0.00
nesta_case9_wscc	5296.69	1.52	0.17	0.00	0.00
nesta_case14_ieee	244.05	5.18	0.28	0.11	0.00
nesta_case24_ieee_rts	63352.20	3.71	0.36	0.01	0.00
nesta_case29_edin	29895.49	0.76	0.16	0.14	0.00
nesta_case30_as	803.13	4.42	0.38	0.06	0.00
nesta_case30_fsr	575.77	1.83	0.50	0.39	0.00
nesta_case30_ieee	204.97	27.91	16.69	15.88	0.00
nesta_case39_epri	96505.52	0.96	0.08	0.05	0.01
nesta_case57_ieee	1143.27	1.59	0.27	0.06	0.00
nesta_case73_ieee_rts	189764.08	3.56	0.36	0.03	0.00
nesta_case89_pegase	5819.81	1.50	0.36	0.17	0.00
nesta_case118_ieee	3718.64	7.87	2.43	2.07	0.06
nesta_case162_ieee_dtc	4230.23	15.44	4.43	4.03	1.08
nesta_case189_edin	849.29	—	1.79	0.21	0.07
nesta_case300_ieee	16891.28	—	3.65	1.18	0.08
nesta_case1354_pegase	74069.35	1.36	0.20	0.08	0.00*
nesta_case1394sop_eir	1366.81	7.31	1.25	0.82	—
nesta_case1397sp_eir	3888.99	5.55	err.	0.93	—
nesta_case1460wp_eir	4640.18	41.26	1.25	0.89	—
nesta_case2224_edin	38127.69	8.45	6.33	6.09	1.22
nesta_case2383wp_mp	1868511.78	5.35	1.38	1.05	0.37
nesta_case2736sp_mp	1307883.11	2.44	0.46	0.30	0.00*
nesta_case2737sop_mp	777629.29	1.75	0.39	0.25	0.00*
nesta_case2746wp_mp	1631775.07	3.09	0.53	0.32	0.00*
nesta_case2746wop_mp	1208279.78	2.50	0.56	0.37	0.00*
nesta_case2869_pegase	133999.29	1.16	0.19	0.09	0.00*
nesta_case3012wp_mp	2600842.72	—	5.18	1.02	err.
nesta_case3120sp_mp	2145739.40	—	5.26	0.55	err.
nesta_case3375wp_mp	7435697.48	—	2.01	0.52	err.
nesta_case9241_pegase	315913.26	—	2.16	—	—

Table 12: AC-OPF Bounds on the NESTA Test Cases (★ - solver reported numerical accuracy warnings).

5.2 Building More Challenging Test Cases

The first goal of NESTA is to establish a comprehensive archive of transmission system test cases with reasonable network parameter values. However, its secondary goal is to serve as a basis for building modified networks for testing a variety of power system scenarios and applications. In this section we demonstrate two of many possible ways that NESTA and the models developed in this report can be used to build interesting new test cases.

It was observed in [11, 39] that power flow congestion is a key component in interesting AC-OTS test cases. This observation inspires the following approach to building congested NESTA test cases. For each of the standard NESTA cases, we make the generator capabilities unbounded and then solve an

active power increase optimization problem, which increases the active power demands proportionally throughout the network until the line thermal limits are binding. Once a maximal increase in active power demand is determined, the set-points of the generators and loads specify an AC power flow test case. The statistical models, AG-Stat, RG-AL50, and AC-Stat are then applied to these new power flow test cases to produce the Active Power Increase (API) test cases. The optimization gaps of these test cases is detailed in Table 13. Interestingly, the congestion introduced by increasing the active power demands leads to significant optimality gaps.

Test Case	\$/h AC	Optimality Gap (%)			
		CP	NF+LL	SOC	SDP
nesta_case3_lmbd_api	367.74	14.79	8.16	3.30	1.26
nesta_case4_gs_api	767.27	6.72	0.77	0.65	0.00
nesta_case5_pjm_api	2998.54	0.75	0.45	0.45	0.00
nesta_case6_c_api	814.40	2.74	0.41	0.35	0.00
nesta_case6_ww_api	273.76	17.17	13.64	13.33	0.00*
nesta_case9_wscc_api	656.60	16.01	0.52	0.00	0.00
nesta_case14_ieee_api	325.56	8.89	1.78	1.34	0.00
nesta_case24_ieee_rts_api	6421.37	24.12	21.14	20.70	1.45
nesta_case29_edin_api	295782.68	0.75	0.44	0.44	err.
nesta_case30_as_api	571.13	8.01	5.14	4.76	0.00
nesta_case30_fsr_api	372.14	48.80	46.19	45.97	11.06
nesta_case30_ieee_api	415.53	12.75	1.48	1.01	0.00
nesta_case39_epri_api	7466.25	13.31	3.71	2.99	0.00
nesta_case57_ieee_api	1430.65	3.51	0.46	0.21	0.08
nesta_case73_ieee_rts_api	20123.98	17.83	15.63	14.34	4.29
nesta_case89_pegase_api	4288.02	22.60	20.71	20.43	18.11
nesta_case118_ieee_api	10325.27	49.69	44.35	44.08	31.50
nesta_case162_ieee_dtc_api	6111.68	19.39	1.97	1.34	0.85
nesta_case189_edin_api	1982.82	—	8.21	5.78	0.05
nesta_case300_ieee_api	22866.01	—	1.81	0.84	0.00
nesta_case1354_pegase_api	59920.94	3.33	0.74	0.56	0.20*
nesta_case1394sop_eir_api	3176.26	15.07	err.	1.58	—
nesta_case1397sp_eir_api	5983.48	10.13	err.	1.59	—
nesta_case1460wp_eir_api	6262.09	9.32	1.26	0.87	—
nesta_case2224_edin_api	46235.43	9.07	2.90	2.77	1.10
nesta_case2383wp_mp_api	23499.48	3.10	1.24	1.12	0.10
nesta_case2736sp_mp_api	25437.70	3.89	1.45	1.33	0.07
nesta_case2737sop_mp_api	21192.40	4.62	1.20	1.06	0.00
nesta_case2746wp_mp_api	27291.58	2.31	0.68	0.58	0.00
nesta_case2746wop_mp_api	22814.86	1.87	0.59	0.49	0.00
nesta_case2869_pegase_api	96573.10	5.16	1.68	1.49	0.92*
nesta_case3012wp_mp_api	27917.36	—	3.51	0.90	err.
nesta_case3120sp_mp_api	22874.98	—	6.26	3.03	err.
nesta_case3375wp_mp_api	48898.95	—	2.08	err.	0.00*
nesta_case9241_pegase_api	241975.18	—	3.12	2.59	—

Table 13: AC-OPF Bounds on the NESTA-API Test Cases (★ - solver reported numerical accuracy warnings).

An entirely different approach to modifying the NESTA cases is inspired by the recent lines of research [10, 9, 23] that indicate phase angle difference bounds can have significant impacts on power system optimization approaches. To investigate these impacts, new test cases are constructed in the following

way. For each of the standard NESTA cases, a *small angle difference* optimization problem is solved, which finds the minimum value of θ^Δ that can be applied on all of the lines in the network, while retaining a feasible AC power flow. Once the small, but feasible, value of θ^Δ is determined, the original test case is updated with this value, yielding new optimal power flow test case, which we call the Small Angle Difference (SAD) test cases. The optimality gaps of these test cases are detailed in Table 14. Interestingly, this entirely different approach to making challenging test cases also leads to significant optimality gaps.

Test Case	\$/h AC	Optimality Gap (%)			
		CP	NF+LL	SOC	SDP
nesta_case3_lmbd_sad	5992.72	5.90	5.15	4.28	2.06
nesta_case4_gs_sad	324.02	66.06	4.93	4.90	0.05
nesta_case5_pjm_sad	26423.32	43.95	5.37	3.61	0.00
nesta_case6_c_sad	24.43	6.79	1.43	1.36	0.00
nesta_case6_ww_sad	3149.51	3.27	0.98	0.80	0.00
nesta_case9_wscc_sad	5590.09	6.69	4.20	1.50	0.00
nesta_case14_ieee_sad	244.15	5.22	0.26	0.06	0.00
nesta_case24_ieee_rts_sad	79804.96	23.56	19.44	11.42	6.05
nesta_case29_edin_sad	46933.26	36.79	34.98	34.47	28.44
nesta_case30_as_sad	914.44	16.06	10.78	9.16	0.47
nesta_case30_fsr_sad	577.73	2.17	0.77	0.62	0.07
nesta_case30_ieee_sad	205.11	27.96	6.48	5.84	0.00
nesta_case39_epri_sad	97219.04	1.69	0.57	0.11	0.09
nesta_case57_ieee_sad	1143.88	1.64	0.32	0.11	0.02
nesta_case73_ieee_rts_sad	235241.70	22.21	16.49	8.37	4.10
nesta_case89_pegase_sad	5827.01	1.62	0.48	0.28	0.03
nesta_case118_ieee_sad	4324.17	20.77	14.34	12.89	7.57
nesta_case162_ieee_dtc_sad	4369.19	18.13	7.47	7.08	3.65
nesta_case189_edin_sad	914.61	—	7.92	2.25	1.20*
nesta_case300_ieee_sad	16910.23	—	3.75	1.26	0.13
nesta_case1354_pegase_sad	74072.33	1.37	0.20	0.08	0.00*
nesta_case1394sop_eir_sad	1577.59	19.69	12.83	11.93	—
nesta_case1397sp_eir_sad	4582.08	19.84	—	14.04	—
nesta_case1460wp_eir_sad	5367.75	49.22	err.	1.08	—
nesta_case2224_edin_sad	38385.14	9.06	6.61	6.18	1.22
nesta_case2383wp_mp_sad	1935308.12	8.62	4.48	4.00	1.30
nesta_case2736sp_mp_sad	1337042.77	4.56	2.51	2.34	2.18*
nesta_case2737sop_mp_sad	795429.36	3.95	2.57	2.42	2.24*
nesta_case2746wp_mp_sad	1672150.46	5.43	2.73	2.44	2.41*
nesta_case2746wop_mp_sad	1241955.30	5.14	3.14	2.94	2.71*
nesta_case2869_pegase_sad	134087.47	1.22	0.25	0.15	0.04*
nesta_case3012wp_mp_sad	2635451.29	—	6.36	2.12	err.
nesta_case3120sp_mp_sad	2203807.23	—	7.33	2.79	err.
nesta_case3375wp_mp_sad	7436381.61	—	2.02	0.52	—
nesta_case9241_pegase_sad	315932.06	—	2.17	1.75	—

Table 14: AC-OPF Bounds on the NESTA-SAD Test Cases (★ - solver reported numerical accuracy warnings).

In both Table 13 and Table 14, the significant optimality gaps may be caused by the non-convexities in the AC-OPF, which the relaxations do not capture, or by the AC heuristic finding local optimal solutions [7]. In either case, these modified test cases present interesting challenges for optimization algorithms.

6 Conclusions

This report has highlighted the shortcomings of using existing test cases for studies of the AC Optimal Power Flow problem, and has proposed data driven models for improving these test cases. The resulting test case archive, NESTA, has reasonable values for key power network parameters, including generation capabilities, costs, and line thermal limits. Our validation demonstrates that many of the NESTA networks have significant optimality gaps, and are therefore interesting AC-OPF test cases. Furthermore, two congested network case studies illustrated how NESTA and the proposed data driven models can be used as building blocks for constructing more challenging AC power flow optimization test cases.

It is important to note that while the research community's primary challenge has been to acquire the real-world data necessary to solve classic academic AC-OPF test cases, this is just the beginning of the data required for comprehensive studies of AC power flow optimization problems [44]. Whenever possible the research community should try to acquire additional data such as: information about configurable assets including bus shunts, switches, and transformer tap settings; the N-1 contingency cases of interest to the network operator and designers; additional line thermal limits for short and long term overloading; ZIP load models; time series data for loads; and detailed generator models including historical market bids, ramp rates, startup/shutdown costs, and power capability curves. Some of these details are available in the EIRGrid dataset [14] and the PES OPF Competition [29], however they were not included in NESTA as the MATPOWER test case file format does not support these additional details.

Although NESTA has significant advantages over other readily available test cases, it is still far from a detailed real-world network specification. This report has highlighted the need for deeper industry engagement for the development of more modern, detailed, and realistic test cases. We hope that NESTA may serve as a stop gap for the research community to study various power system optimization problems, while more real-world test cases are being developed.

7 Acknowledgements

NICTA is funded by the Australian Government through the Department of Communications and the Australian Research Council through the ICT Centre of Excellence Program.

References

- [1] O. Alsac and B. Stott. Optimal load flow with steady-state security. *IEEE Transactions on Power Apparatus and Systems*, PAS-93(3):745–751, May 1974.
- [2] Xiaoqing Bai, Hua Wei, Katsuki Fujisawa, and Yong Wang. Semidefinite programming for optimal power flow problems. *International Journal of Electrical Power & Energy Systems*, 30(67):383 – 392, 2008.
- [3] Russell Bent, Carleton Coffrin, Rodrigo Gumucio, and Pascal Van Hentenryck. Transmission network expansion planning: Bridging the gap between ac heuristics and dc approximations. *Proceedings of the 18th Power Systems Computation Conference (PSCC'14)*, Wroclaw, Poland, 2014.
- [4] G.W. Bills. On-line stability analysis study, rp 90-1. Request online at <http://www.osti.gov/scitech/biblio/5984031>, Oct 1970.
- [5] Seth Blumsack. *Network Topologies and Transmission Investment Under Electric-Industry Restructuring*. PhD thesis, Carnegie Mellon University, 2006.
- [6] W. A. Bukhsh and Ken McKinnon. Network data of real transmission networks. Published online at <http://www.maths.ed.ac.uk/optenergy/NetworkData/>, 2013. Accessed: 17/07/2014.
- [7] W.A. Bukhsh, A. Grothey, K.I.M. McKinnon, and P.A. Trodden. Local solutions of the optimal power flow problem. *IEEE Transactions on Power Systems*, 28(4):4780–4788, Nov 2013.
- [8] Waqqas A. Bukhsh. Test case archive of optimal power flow (opf) problems with local optima. Published online at <http://www.maths.ed.ac.uk/0ptEnergy/LocalOpt/>, May 2013. Accessed: 25/08/2014.
- [9] Coffrin Carleton and Pascal Van Hentenryck. A linear-programming approximation of ac power flows. *Forthcoming in INFORMS Journal on Computing*, 2014.

[10] C. Coffrin, P. Van Hentenryck, and R. Bent. Accurate Load and Generation Scheduling for Linearized DC Models with Contingencies. *Proceedings of the 2012 IEEE Power & Energy Society General Meetings (PES)*, 2012.

[11] Carleton Coffrin, Hassan Hijazi, Karsten Lehmann, and Pascal Van Hentenryck. Primal and dual bounds for optimal transmission switching. *Proceedings of the 18th Power Systems Computation Conference (PSCC'14)*, Wroclaw, Poland, 2014.

[12] M.L. Crow. *Computational Methods for Electric Power Systems*. Electric Power Engineering Series. Taylor & Francis, 2002.

[13] B. Dembart, A.M. Erisman, E.G. Cate, M.A. Epton, and H. Dommel. Power system dynamic analysis: Phase I. Final report. Request online at <http://www.osti.gov/scitech/biblio/7296152>, Jul 1977.

[14] EirGrid. Ten year transmission forecast statement 2013. Published online at <http://www.eirgrid.com/transmission/transmissionforecaststatement/tenyeartransmissionforecaststatement2013/tytfs2013modelfiles/>, 2013. Accessed: 17/07/2014.

[15] M. Farivar, C.R. Clarke, S.H. Low, and K.M. Chandy. Inverter var control for distribution systems with renewables. In *2011 IEEE International Conference on Smart Grid Communications (SmartGridComm)*, pages 457–462, Oct 2011.

[16] C.M. Ferreira, F.P.M. Barbosa, and C.I.F. Agreira. Transient stability preventive control of an electric power system using a hybrid method. In *Power System Conference, 2008. MEPCON 2008. 12th International Middle-East*, pages 141–145, March 2008.

[17] R. W. Ferrero, S. M. Shahidehpour, and V. C. Ramesh. Transaction analysis in deregulated power systems using game theory. *IEEE Transactions on Power Systems*, 12(3):1340–1347, Aug 1997.

[18] E.B. Fisher, R.P. O'Neill, and M.C. Ferris. Optimal transmission switching. *IEEE Transactions on Power Systems*, 23(3):1346–1355, 2008.

[19] S. Fliscounakis, P. Panciatici, F. Capitanescu, and L. Wehenkel. Contingency ranking with respect to overloads in very large power systems taking into account uncertainty, preventive, and corrective actions. *IEEE Transactions on Power Systems*, 28(4):4909–4917, Nov 2013.

[20] J.J. Grainger and W.D. Stevenson. *Power system analysis*. McGraw-Hill series in electrical and computer engineering: Power and energy. McGraw-Hill, 1994.

[21] C. Grigg, P. Wong, P. Albrecht, R. Allan, M. Bhavaraju, R. Billinton, Q. Chen, C. Fong, S. Haddad, S. Kuruganty, W. Li, R. Mukerji, D. Patton, N. Rau, D. Reppen, A. Schneider, M. Shahidehpour, and C. Singh. The ieee reliability test system-1996. a report prepared by the reliability test system task force of the application of probability methods subcommittee. *IEEE Transactions on Power Systems*, 14(3):1010–1020, Aug 1999.

[22] K. Hedman, M. Ferris, R. O'Neill, E. Fisher, and S. Oren. Co-optimization of generation unit commitment and transmission switching with n-1 reliability. In *Power and Energy Society General Meeting, 2010 IEEE*, pages 1–1, July 2010.

[23] H. Hijazi, C. Coffrin, and P. Van Hentenryck. Convex quadratic relaxations of mixed-integer non-linear programs in power systems. Published online at http://www.optimization-online.org/DB_HTML/2013/09/4057.html, 2013.

[24] R.A. Jabr. Radial distribution load flow using conic programming. *IEEE Transactions on Power Systems*, 21(3):1458–1459, Aug 2006.

[25] R.A. Jabr. Optimization of ac transmission system planning. *IEEE Transactions on Power Systems*, 28(3):2779–2787, Aug 2013.

[26] Prabha Kundur. *Power System Stability and Control*. McGraw-Hill Professional, 1994.

[27] J. Lavaei and S.H. Low. Zero duality gap in optimal power flow problem. *IEEE Transactions on Power Systems*, 27(1):92–107, feb. 2012.

[28] Javad Lavaei. Opf solver. Published online at <http://www.ee.columbia.edu/~lavaei/Software.html>, oct. 2014. Accessed: 22/02/2015.

[29] Kwang Y. Lee, Istvan Erlich, Jose L. Rueda, and Sebastian Wildenhues. IEEE PES Competition on Application of Modern Heuristic Optimization Algorithms for Solving Optimal Power Flow Problems. Published online at <http://sites.ieee.org/pes-iss/working-groups/>, September 2013. Accessed: 25/08/2014.

[30] Karsten Lehmann, Alban Grastien, and Pascal Van Hentenryck. AC-Feasibility on Tree Networks is NP-Hard. *IEEE Transactions on Power Systems*, 2015 (to appear).

[31] B.C. Lesieutre, D.K. Molzahn, A.R. Borden, and C.L. DeMarco. Examining the limits of the application of semidefinite programming to power flow problems. In *49th Annual Allerton Conference on Communication, Control, and Computing (Allerton)*, 2011, pages 1492 –1499, sept. 2011.

[32] Fangxing Li and Rui Bo. Small test systems for power system economic studies. In *Power and Energy Society General Meeting, 2010 IEEE*, pages 1–4, July 2010.

[33] Richard Lincoln. Pylon 0.4.4, port of matpower to python. Published online at <http://pypi.python.org/pypi/Pylon>. Accessed: 25/08/2014.

[34] J.A. Momoh, R. Adapa, and M.E. El-Hawary. A review of selected optimal power flow literature to 1993. i. nonlinear and quadratic programming approaches. *IEEE Transactions on Power Systems*, 14(1):96 –104, feb 1999.

[35] J.A. Momoh, M.E. El-Hawary, and R. Adapa. A review of selected optimal power flow literature to 1993. ii. newton, linear programming and interior point methods. *IEEE Transactions on Power Systems*, 14(1):105 –111, feb 1999.

[36] J. R. Avalos Munoz. *Analysis and Application of Optimization Techniques to Power System Security and Electricity Markets*. PhD thesis, University of Waterloo, 2008.

[37] Richard P. O'Neill, Anya Castillo, and Mary B. Cain. The iv formulation and linear approximations of the ac optimal power flow problem. Published online at <http://www.ferc.gov/industries/electric/indus-act/market-planning/opf-papers/acopf-2-iv-linearization.pdf>, December 2012. Accessed: 18/11/2013.

[38] A. Pai. *Energy Function Analysis for Power System Stability*. Kluwer international series in engineering and computer science. Springer, 1989.

[39] T. Potluri and K.W. Hedman. Impacts of topology control on the acopf. In *Power and Energy Society General Meeting, 2012 IEEE*, pages 1–7, 2012.

[40] Power Systems Control and Automation Laboratory. Ieee 24-substation reliability test system, generator data. Published online at <http://pscal.ece.gatech.edu/testsys/generators.html>. Accessed: 22/10/2013.

[41] Power Systems Engineering Research Center. Transfer capability calculator. Published online at <http://www.pserc.cornell.edu/tcc/>, 2001. Accessed: 25/08/2014.

[42] K Purchala, L Meeus, D Van Dommelen, and R Belmans. Usefulness of DC power flow for active power flow analysis. *Power Engineering Society General Meeting*, pages 454–459, 2005.

[43] B Stott, J Jardim, and O Alsac. Dc power flow revisited. *IEEE Transactions on Power Systems*, 24(3):1290–1300, 2009.

[44] Brian Stott and Ongun Alsac. Optimal power flow — basic requirements for real-life problems and their solutions. self published, available from brianstott@ieee.org, Jul 2012.

[45] P.M. Subcommittee. Ieee reliability test system. *IEEE Transactions on Power Apparatus and Systems*, PAS-98(6):2047–2054, Nov 1979.

[46] K. C. Toh, M.J. Todd, and R. H. Ttnc. Sdpt3 – a matlab software package for semidefinite programming. *OPTIMIZATION METHODS AND SOFTWARE*, 11:545–581, 1999.

[47] University of Washington, Dept. of Electrical Engineering. Power systems test case archive. Published online at <http://www.ee.washington.edu/research/pstca/>, 1999. Accessed: 30/04/2012.

[48] U.S. Energy Information Administration. Annual electric generator data - eia-860 data file. Published online at www.eia.gov/electricity/data/eia860/, 2012. Accessed: 25/08/2014.

- [49] U.S. Energy Information Administration. State energy data system (seds): 1960-2012 (complete). Published online at <http://www.eia.gov/state/seds/seds-data-complete.cfm>, 2012. Accessed: 25/08/2014.
- [50] U.S. Energy Information Administration. Table of fuel codes. Published online at <http://www.eia.gov/electricity/data/browser/dataservice/termsAndDefs.cfm?topic=1&showDetail=true&showFilterValues=true>, 2014. Accessed: 25/08/2014.
- [51] Abhinav Verma. *Power Grid Security Analysis : An Optimization Approach*. PhD thesis, Columbia University, 2009.
- [52] A. Wächter and L. T. Biegler. On the implementation of a primal-dual interior point filter line search algorithm for large-scale nonlinear programming. *Mathematical Programming*, 106(1):25–57, 2006.
- [53] A.J.W.B. Wollenberg. *Power Generation Operation & Control*. Wiley India Pvt. Limited, 2006.
- [54] R.D. Zimmerman, C.E. Murillo-S andnchez, and R.J. Thomas. Matpower: Steady-state operations, planning, and analysis tools for power systems research and education. *IEEE Transactions on Power Systems*, 26(1):12 –19, feb. 2011.